JOURNAL OF APPLIED POLYMER SCIENCE VOL. 19, PP. 983-998 (1975)

Thermal Degradation of Polymers. IX. Ablation Studies on Composites: Comparison of Laboratory Test Methods with Tethered Rocket Motor Firings

D. KERSHAW* and R. H. STILL, *Department of Polymer and Fibre Science, UMIST, Manchester, England,* and V. G. BASHFORD, *Polymer Technology Department, Manchester Polytechnic, Manchester, England*

Synopsis

The use of a novel laboratory ablation test rig for material selection is described. The results obtained are compared with those obtained from differential thermal analysis, thermogravimetry, and tethered rocket motor test firings.

INTRODUCTION

In two previous papers,[1,2] we described a laboratory ablation test rig for use with tubular composite specimens. Composites based on commercially available high-temperature resins with asbestos as the reinforcing phase and composites based on a standard phenolic resin and various fibrous reinforcing materials were assessed for use in rocket motor applications.

Ablation resistance, smoke, and flash measurements were made and correlated with composite structure. We now report comparative studies of these materials using the laboratory test rig, thermoanalytical techniques of DTA and TG, and tethered rocket motor firings.

EXPERIMENTAL

Apparatus

The laboratory ablation test rig and operating procedure is as previously described.[1,3]

Thermoanalytical Studies

Thermoanalytical studies were made on a Stanton TRO 1 thermobalance fitted with an STA attachment, which allowed the simultaneous recording of both differential thermal analysis (DTA) and thermogravimetric analysis (TG) data on the same sample.

A heating rate of 5°C/min (nominal) was used for all DTA/TG determinations. Calcined alumina was used as the inert reference material for DTA

* Present address: Kelvin Lenses, Ltd., Denton, Manchester, England.

© 1975 by John Wiley & Sons, Inc.

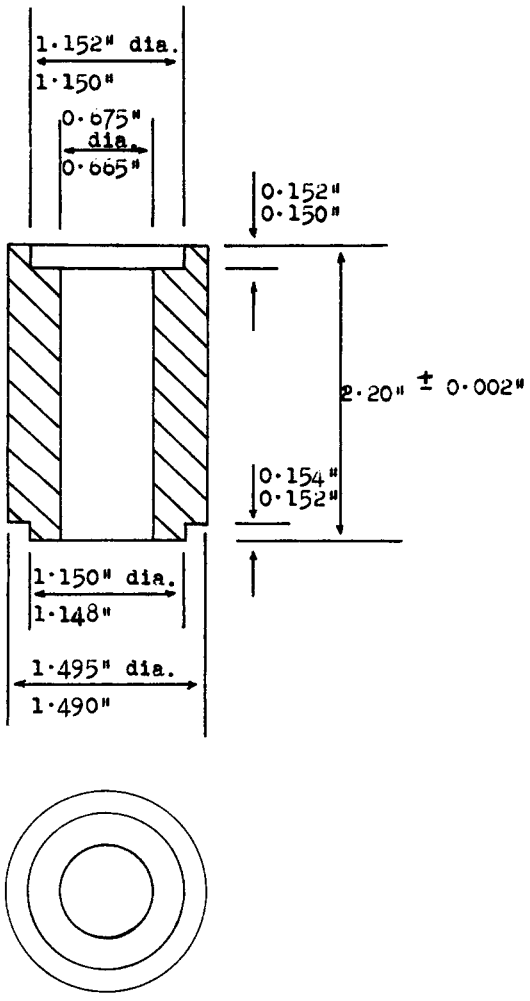

Fig. 1. Field trial specimen dimensions.

studies and samples were contained in platinum crucibles ($^1/_4$ in. o.d. × $^5/_{16}$ in. deep) dimped to accept the thermocouple probes.

Pure white spot nitrogen was used as the degradation atmosphere, and the gas flow was arranged to flow up over the crucible at 400 ml/min.

All temperatures recorded are sample temperatures, and all thermograms have been corrected for buoyancy effects.

Isothermal weight loss studies were made on the Stanton TRO 1 balance/STA attachment in the following manner. The DTA attachment was not operated during isothermal studies, and the two dimped crucibles were replaced by a single larger platinum crucible.

The following technique was utilized to rapidly load the test samples into the crucible to minimize furnace heat losses. A nonablating 80-mg steel pellet in the crucible to be used was initially employed to produce the baseline trace at the operating temperature. This pellet was then removed and the furnace and crucible allowed to reequilibriate with the thermobalance returned to the rest position.

The furnace was quickly raised, an 80-mg pellet specimen placed in the crucible, and the furnace lowered again, the thermobalance recording mechanism being switched on at the same time. Each specimen was subjected to pyrolysis for a 60-min period in a nitrogen atmosphere.

Sample Preparation for Thermal Analysis

The composite specimens were produced from 1-in. off-cut samples from the molded tubes. The fibrous reinforcement materials were tested in the "as received" state. All resins were assessed in the fully cured state. Resins giving off volatile cure reaction products were compression molded into discs $1^1/_2$ in. diam. $\times$ $^1/_4$ in. thick. Resins which did not give off volatile cure reaction products were cast in silicone rubber molds which overcame the problem of resin leakage normally encountered when compression molding low-viscosity resins at elevated temperatures. Curing and postcuring (where applicable) were carried out as previously described.[1]

Field Trial Studies

Sample Preparation. Cylindrical moldings $2^1/_2$ in. diam. $\times$ $2^1/_2$ in. deep were produced. Molding compounds were prepared as previously described,[1,2] and preforms (320 g) $2^1/_2$ in. diam. $\times$ $2^3/_4$ in. deep were produced. These preforms were preheated prior to molding using a Radyne high-frequency unit. The phenolic materials were preheated for 1 min at 0.5 KW, the polyimide and polyphenylene materials for $1^1/_2$ min at 0.5 KW. The materials were then compression molded and cured as previously described for the tubular specimens.[1,2]

The cured billets were machined to produce tubular field specimens of the dimension shown diagramatically in Figure 1. Three such specimens were then fitted together as shown in Figure 2 between standard Durestos RA51 end pieces. The specimens were fitted with thermocouples to monitor material temperatures during the test. Details of the specimen arrangements and thermocouple depths are shown in Table I. The samples were finally assembled into a single cylinder test motor as shown in Figure 3.

Test Procedure. The test motors were fired for a nominal 25 sec and then flushed with nitrogen for 5 min to allow the specimens to cool in a nonoxidizing atmosphere. Prior to removing the specimens from the blast tube, the tube was filled with a room-temperature curing epoxy resin. The specimens were then

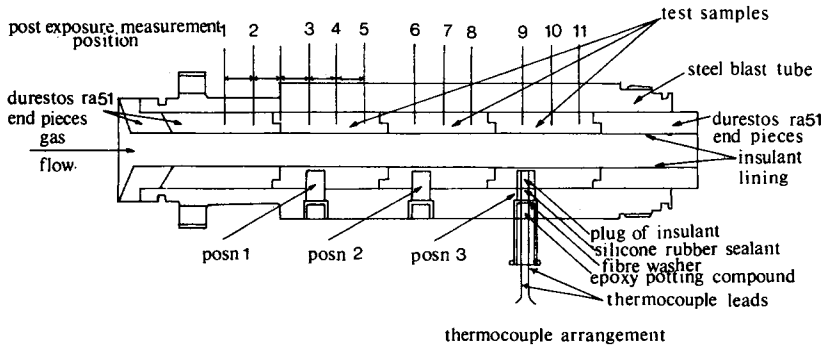

Fig. 2. Lined blast tube.

TABLE I
Tethered Rocket Motor Specimen Arrangement

Material[a]	Posn	Thermocouple depths, in. da	db	dc	Trial no./firing time, sec
A/Phenolic resin CS303	1	0.117	0.080	0.040	1/25.1
Durestos RA51 control	2	0.118	0.080	0.040	
A/Phenolic resin CS311	3	0.118	0.079	0.040	
A/Polyimide P13N	1	0.117	0.080	0.040	
Durestos RA51 control	2	0.120	0.080	0.038	2/25.1
A/Xylok 210	3	0.119	0.080	0.038	
Refrasil/Resin RA51	1	0.103	0.066	0.026	
Durestos RA51 control	2	0.107	0.066	0.026	3/24.5
Kaowool/Resin RA51	3	0.107	0.063	0.026	

[a] A = Asbestos FR91.

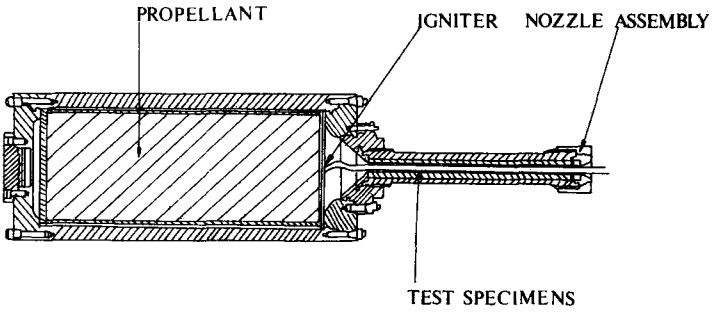

Fig. 3. Typical rocket motor assembly.

removed from the blast tube, sectioned, and polished. Char depths and virgin material remaining after test were measured by means of a traveling microscope.

RESULTS AND DISCUSSION

The ablation test rig developed for these studies utilizes tubular specimens to simulate the rocket motor exhaust situation, and to simultaneously obtain information on smoke evolution, flash, and ablation behavior. The rig is cheap to operate, and as such is a very useful screening device for the initial evaluation of new materials.

This new method has several advantages over the standard method for oxy-acetylene ablation testing of thermal insulation materials[4] and the NOL alpha rod test.[5] These are that atmospheric oxidation is prevented, much less surface erosion occurs, and the operating conditions, with the flame passing through the tubular specimen rather than impinging on a flat surface, more correctly simulates the rocket motor blast tube situation.

In addition, smoke and flash data are produced which are not available from the other methods.

To obtain these advantages, a different flame source, oxy-acetylene ratio, and gas flow rate are used. The flame produced on the rig is of larger diameter initially emerging from a series of 17 holes ($^1/_{32}$ in. diam.) set in two circles $^1/_4$ and $^1/_2$ in. in diameter in the torch tip. This is markedly different to the single $^1/_8$-

in. diameter orifice used in the standard ablation test method. As a result of the different oxy-acetylene ratios, the test rig flame is at a slightly lower temperature, 3080°C, as compared with the standard flame of 3260°C.[4] The effect of flow rate differences which are significantly different at 120 cu ft/hr for the rig and 225 cu ft/hr for the standard is also of major importance. This means that the total heat flux to the material surface will differ. This arises both as a result in the differences in gas flow and as a result of the flame passing along the inside surface of the tubular specimen rather than impinging directly onto a flat surface.

In an attempt to measure the heat flux, various inert nonablating tubular specimens were investigated. The most reproducible results were obtained using a graphite tube of the same dimensions as the test specimen. The heat flux was calculated for the rig and for a 1800°C, 580 psi rocket motor using the equation given in the standard ASTM method.[4] The results indicate a heat flux of 1.74 W/cm^2 for the rig and of 92 W/cm^2 for the rocket motor which may be compared with the reported value of 520 ± 60 W/cm^2 (the quoted specification limits of the ASTM standard method).

Thus, while it can be seen that the heat flux is very low compared with the flat-plate method, this ASTM method would appear to be very high as compared with the rocket motor system used to further assess the samples tested on the rig. In addition, the method used to evaluate the heat flux in the rig was subject to high heat loss errors in comparison to the sophisticated water-cooled calorimeter used in the ASTM method.

That the method used on the rig is justified is further borne out by comparative studies on the rig and those utilizing the rocket motors, where the same features are observed (see later section). Further to this, the major advantage of the method lies in the ability to screen materials without costly tethered rocket motor trials and to readily obtain data on smoke and flash unavailable from either the rocket motor, the standard oxy-acetylene method, or the NOL alpha rod test.

Thermoanalytical Studies

Thermogravimetric analysis (TG) is normally carried out on particulate samples. In this investigation, it was considered that "bulk" specimens would better simulate the service conditions of both the rocket motor and the test rig specimens. In addition, the use of a "bulk" specimen facilitated the study of these materials since there are numerous problems associated with the production of reproducible mesh-size particulate samples from fiber-reinforced composites by grinding.

Preliminary studies in air showed that the thermo-oxidative degradation of the control phenolic resin was complete between 700° and 800°C depending upon the surface area of the sample. A residue of 4–5% which resulted from the zinc stearate lubricant in the resin was found in all cases. This complete breakdown of the resin in air is in contrast to service requirements where a good char structure is considered to be essential for good ablation performance. In addition, simultaneous TG/DTA showed these reactions to be highly exothermic, which completely masked any other reactions occurring in the system.

Accordingly, attention was turned toward a nonoxidative atmosphere in which to carry out these studies. The gas atmosphere operative in a typical rocket

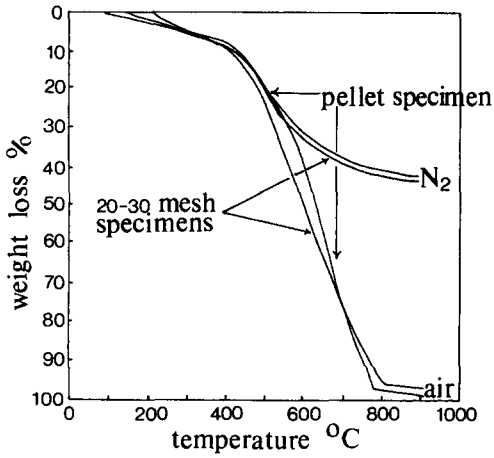

Fig. 4. Thermograms of cured resin RA51 in air and nitrogen. Sample form and weight: pellet (air), 84.3 mg; pellet (N_2), 76.2 mg; 20–30 mesh powder (air), 59.3 mg; 20–30 mesh powder (N_2), 83.0 mg.

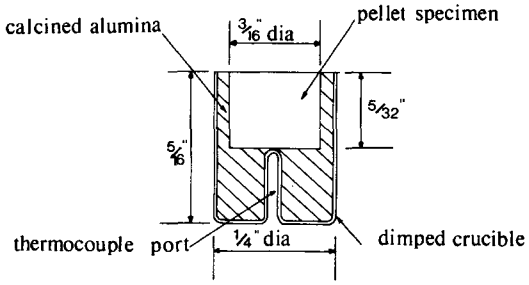

Fig. 5. Pellet specimen arrangement.

motor[6] is a complex mixture typically containing, in volume fraction terms, carbon monoxide 0.33, carbon dioxide 0.17, water 0.17, hydrogen 0.19, nitrogen 0.12, other constituents 0.02. In view of this, nitrogen was chosen as a safe alternative compromise atmosphere.

In Figure 4, TG curves obtained from a pellet specimen ($^3/_{16}$ in. diam. and $^5/_{32}$ in. deep) and a 20–30-mesh specimen of cured phenolic resin RA51 are compared in air and nitrogen atmospheres. The results indicate that a char residue in excess of 55% was obtained in nitrogen irrespective of the specimen surface area. In air, the procedural decomposition temperature (P.D.T.) (the temperature at which weight loss becomes measurable) is lower for the specimen of higher surface area.

In view of the results in nitrogen and on the basis of handleability and ease of preparation, an 80-mg pellet sample was adopted for all runs. The specimen was packed in alumina in the crucible, as shown in Figure 5, in an attempt to further simulate the one-dimensional heat flow experienced under service conditions.

The char yield results obtained for all materials studied are shown in Table II. In all cases except for the resin RA51/PAN, the isothermal weight loss results and those obtained from dynamic thermogravimetry correlate very well. This

TABLE II
Char Yields from Thermogravimetry in a Dynamic Nitrogen Atmosphere

Material[a]	% Char yield, at 900°C dynamic TG[b]	% Char yield, isothermal TG at 800°C	% Char yield as measured on test rig[c]
Durestos RA51 control	71.0	70.6	72.0
A/Phenolic resin CS303	73.4	71.9	76.3
A/Phenolic resin CS303 (postcured)	76.2	71.7	76.6
A/Phenolic resin CS311	73.8	71.9	73.4
A/Phenolic resin CS311 (postcured)	74.0	70.1	76.2
A/Polyimide P13N	74.0	70.1	73.7
A/Polyimide QX13	71.2	71.2	72.6
A/Polyphenylene 1711	77.3	74.4	74.6
A/Xylok 210	70.5	70.0	76.3
A/Epoxy 154/NMA/BDMA	65.9	59.0	72.0
A/Epoxy 4617/DDM	59.9	56.5	67.6
A/Polyester 17449	59.9	55.3	68.4
A/Silicone MS2106	77.5	79.5	—
Refrasil/resin RA51	77.6	78.7	81.2
Kaowool/resin RA51	83.4	81.0	80.5
E Glass/resin RA51	83.9	81.2	80.3
Carbon fiber HM-S/resin RA51	80.4	78.1	79.2
Carbon fiber A/resin RA51	80.2	79.2	74.3
PAN/resin RA51	50.6	28.4 31.2	45.1

[a] A = Asbestos.
[b] Heating rate 5°C/min (nominal).
[c] Measured by weight loss.

suggests that the amount of char residue formed is essentially independent of the heating rate applied to the sample in the range studied. The values obtained by the isothermal weight loss studies are usually lower than those by dynamic TG, suggesting that further curing or cyclization reactions occur during the slower heating up of the sample which do not occur under isothermal conditions at 800°C. The magnitude of such effects is, however, small. The isothermal method is a much more rapid screening method with weight loss being complete in a few minutes compared with a 4-hr heating cycle of the TGA furnace followed by a cooling cycle. Isothermal studies, therefore, provide a rapid and low-cost method of screening possible materials for rig testing since they may be carried out with a simple furnace and conventional balance.

The results obtained must, however, be treated with caution. While it is true to say that materials exhibiting low char yields, <70%, do not exhibit good ablative properties, the converse is not true. The silicone material which failed under the rig test conditions is typical of this behavior showing a high char yield on TG. The failure on the rig may be ascribed to mechanical inadequacy of char residue. In other cases where char yields are high but the overall ablation performance is poor, this may be ascribed to one of the following properties of the char: (a) poor insulant performance, (b) poor erosion resistance, and (c) the absence of endothermic cooling reactions of the fibrous reinforcement to reduce the rate of char formation by reducing the sample temperature. Such properties

TABLE III
Char or Residue Yield on Dynamic TG in Nitrogen at 900°C

Material	Further treatment	Char or residue, %
Resin RA51	—	57.5
Resin RA51	dried 2 days at 90°C + 1 day at 120°C	57.5
Resin RA51	postcured 6 hr at 200°C	60.7
Phenolic resin CS303	—	60.8
Phenolic resin CS303	postcured	60.6
Phenolic resin CS311	—	56.0
Phenolic resin CS311	postcured	60.5
Polyimide P13N	—	60.5
Polyimide QX13	—	59.7
Polyphenylene 1711	—	66.4
Xylok 210	—	47.5
Epoxy 154/NMA/BDMA	—	27.4
Epoxy 4617/DDM	—	16.4
Polyester 17449	—	7.6
Silicone MS2106	—	63.8
Asbestos FR91	—	86.5
Refrasil	—	98.7
Kaowool	—	98.7
E Glass	—	98.6
Carbon fiber HM-S	—	99.8
Carbon fiber A	—	95.6
PAN	—	61.0

cannot, however, be assessed by TG and only (c) can be assessed by simple thermoanalytical techniques, i.e., DTA.

In Table II, the "char yields" obtained on the rig are also recorded. These figures serve as a useful guide to "ablation behavior" but they are in no way a correct assessment of char yield. This is because the tested specimen weight will contain in most cases a contribution from the virgin material left after test. In addition, the weight lost includes a contribution due to erosion of the char as well as the volatiles lost on char formation. A more realistic assessment is gained from studies of the char and virgin thicknesses.

In addition to the TG studies made on the composites, the individual components, i.e., the resins and the fibers, were also subjected to dynamic TG as shown in Table III. It can be seen that these materials show a similar pattern to that observed with the composite materials. The results in Table II are in the correct order on the basis of the concentration of each component present in the composite indicating little interactive effect between the fibrous reinforcement and the resin during the char formation stage.

An anomalous result is that for the Xylok 210 resin, which suggests that in the composite some protection of the resin is afforded by the asbestos. This possibly occurs by allowing further curing of the resin as a result of the cooling effect of the water loss. The results on the phenolic control resin subjected to drying and curing cycles show some slight differences. The drying cycle used is that recommended to aid long-term storage stability. It does not increase char yield but merely increases the P.D.T. from 100° to 140°C. The postcured sample,

however, shows a slightly higher char yield, indicating that further crosslinking has occurred in the system.

Differential Thermal Analysis

DTA was carried out simultaneously with dynamic TG studies. The results obtained, in general, were difficult to interpret in that there was considerable baseline drift effect due to the magnitude of the change in thermal character of the initial sample and that of the char as it formed. This resulted in difficulty in assessing the exact course of the degradation process. In an attempt to overcome this problem, the alumina used as the inert reference material was replaced by a charred pellet sample. This partially solved the problem, but at temperatures in excess of 700°C the problem again arose making interpretation difficult.

In addition, it should be noted that the equipment used necessitated that these runs were made under conditions more suitable for TG analysis.

Thermograms shown in Figures 6 and 7 are illustrative of the information to be gained from this technique for ablation studies. Figure 6 shows the thermogram of the asbestos fiber used as a reinforcing agent in much of this work. The thermogram shows an endothermic deviation starting at 410°C, a major endotherm at peak minimum 710°C, and a sharp exotherm at peak maximum 840°C. This type of behavior has been reported previously[7] and has been interpreted as being due to (a) reversible loss of loosely bound water, (b) loss of more rigidly bound water of crystallization, and (c) a structural change from the crysotile to the crystalline olivine form of asbestos. The two endothermic processes (a) and (b), which amount to 13.5% weight loss of the asbestos component of the reinforced composite, explain the superior behavior of asbestos as an ablative cooling

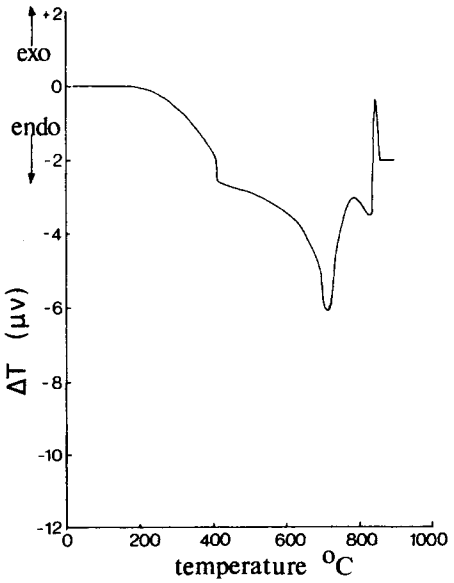

Fig. 6. DTA trace for asbestos fiber: sample weight, 48 mg; furnace atmosphere, N_2 at 400 ml/min; heating rate, 5°C/min (nominal).

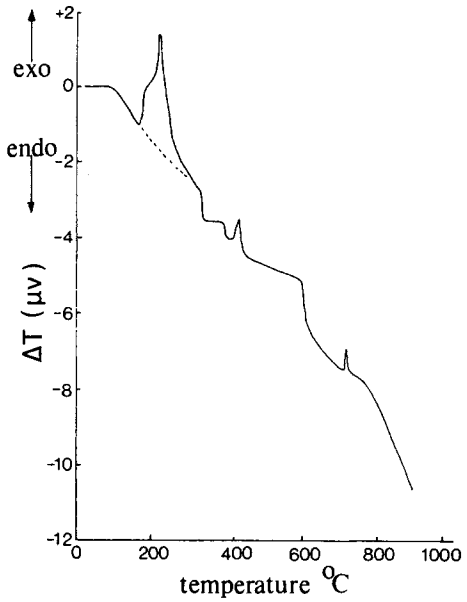

Fig. 7. DTA trace for resin RA51/polyacrylonitrile composite: sample weight, 80 mg (pellet); furnace atmosphere, N_2 at 400 ml/min; heating rate, 5°C/min (nominal).

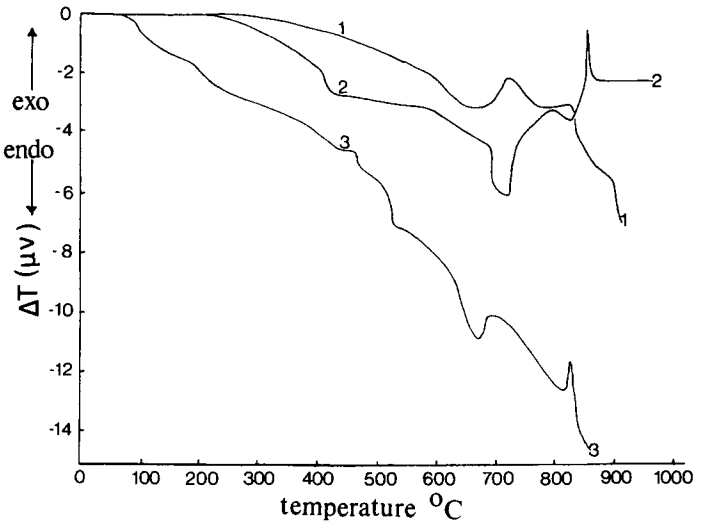

Fig. 8. DTA traces for polyimide QX13 (3) and polyphenylene 1711 (1) composites with asbestos, and asbestos flock (2). Composites: sample weight, 80 mg (pellet); asbestos flock sample weight, 48 mg; furnace atmosphere, N_2 at 400 ml/min; heating rate, 5°C/min (nominal).

material as compared with the low-weight-loss fibers shown in Table III. All asbestos composites showed these effects.

The only fiber studied which showed a major weight loss which was bigger than asbestos was PAN. The thermogram for the resin RA51/PAN composite is shown in Figure 7. It exhibits a large exotherm peak maximum, 220°C. This has been reported[8] as being involved with changes in the fiber molecular structure

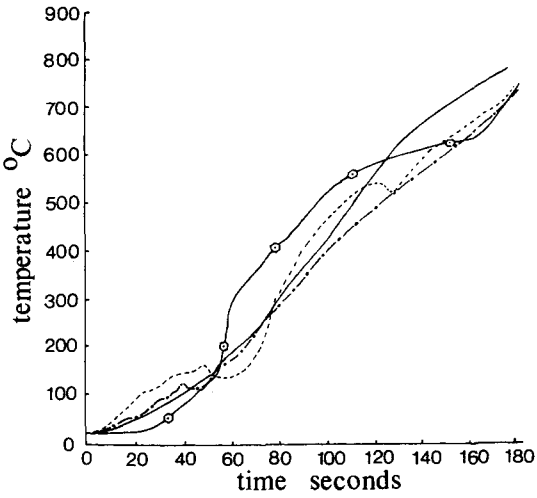

Fig. 9. Ablation test rig time–temperature profiles: (------) A/polyphenylene 1711; (-·-·-) A/polyimide QX13; (———) durestos RA51 control; (—⊙—) polyacrylonitrile/resin RA51; A = asbestos.

involving ring closure. The result shown in Figure 7 explains, in part, the time–temperature profiles obtained on the ablation rig (Fig. 9). In addition, it also explains the unique behavior of this system on TG where it is grossly affected by the heating rate (Table II).

The polyimide QX13 (Fig. 8) shows a broad endotherm commencing at 100°C, which explains the plateau effect found on the time–temperature profile of this composite with asbestos (Fig. 9).

Similarly, the polyphenylene 1711 material (Fig. 8) shows an endotherm, peak minimum 650°C, which explains the second plateau observed in the time–temperature profile for this composite with asbestos (Fig. 9). It may thus be seen that TG and DTA provide useful screening methods for studying the individual components used in composites for ablation studies and the composites themselves. Furthermore, these results on the composites are useful in the interpretation of the results obtained from either rig testing or tethered rocket motor firings.

Field Trial Studies

The materials used for field trial tests were selected on the basis of their performance on the test rig. This was done to evaluate the potential usefulness of the rig test method. All the materials studied showed similar or improved ablation characteristics to the Durestos RA51 control material and improved smoke emission properties. The following materials were subjected to rocket motor firings: asbestos-reinforced composites based on phenolic resins CS303 and 311, polyimide P13N, Xylok 210, and phenolic resin RA51 reinforced with Refrasil and Kaowool. The char thickness results and associated performance data are shown in Table IV.

The time–temperature profiles obtained for the various materials at each thermocouple position are shown in Figures 10, 12, and 14 for the three different firings. It can be seen that the reproducibility of results between firings is not

TABLE IV
Field Trial Results

Firing no.	Material[a]	Initial thickness, in.	Char thickness, in.	Virgin material, in.	Thickness attacked, in.	Attack rate, (in./sec) × 10^3	Erosion rate, (in./sec) × 10^3
	A/CS303	0.412	0.080–0.120	0.210–0.260	0.150–0.200	6.0–8.0	1.0–4.8
1	Durestos RA51 control	0.412	0.060–0.100	0.240–0.310	0.100–0.170	4.0–6.8	0–4.4
	A/CS311	0.412	0.070–0.110	0.230–0.270	0.140–0.180	5.6–7.2	1.2–4.0
	A/Polyimide P13N	0.412	0.060–0.080	0.250–0.290	0.120–0.160	4.8–6.4	1.6–4.0
2	Durestos RA51 control	0.412	0.040–0.090	0.260–0.300	0.110–0.160	4.4–6.4	0.8–4.8
	A/Xylok	0.412	0.060–0.130	0.230–0.250	0.160–0.180	6.4–7.2	1.2–4.8
	Refrasil/resin RA51	0.412	0.130–0.170	0.240–0.280	0.130–0.170	5.3–6.9	0–1.6
3	Durestos RA51 control	0.412	0.070–0.100	0.240–0.280	0.130–0.190	5.3–7.7	1.2–4.9
	Kaowool/resin RA51	0.412	0.120–0.150	0.240–0.250	0.160–0.210	6.5–8.6	0.4–3.7

[a] A = Asbestos.

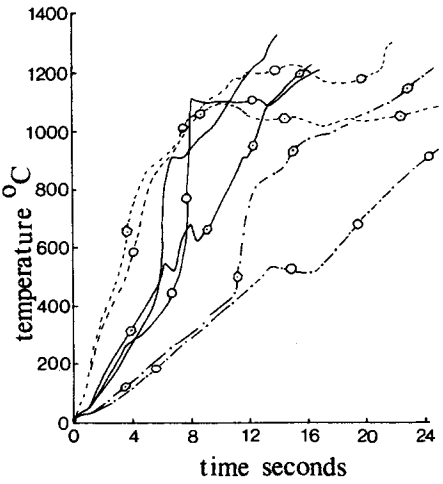

Fig. 10. Tethered rocket time-temperature profiles. Material and thermocouple depth: (----⊙----) A/phenolic CS303, 0.040 in.; (----O----) A/phenolic CS311, 0.040 in.; (—⊙—) A/phenolic CS303, 0.080 in.; (———) Durestos RA51 control, 0.080 in.; (—O—) A/phenolic CS311, 0.079 in.; (-·-⊙-·-) A/phenolic CS303, 0.117 in.; (-·-O-·-) A/phenolic CS311,. 0.118 in.; A = asbestos.

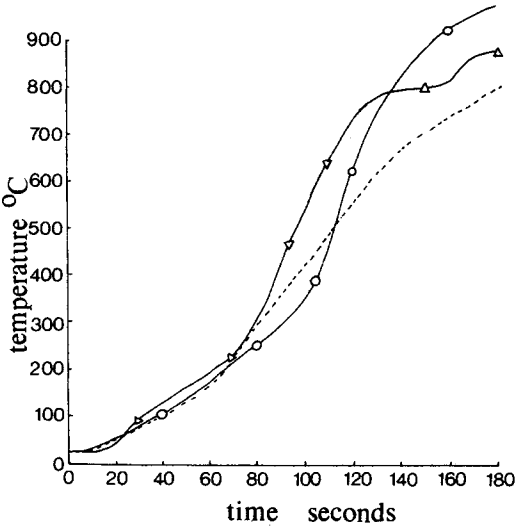

Fig. 11. Ablation test rig time–temperature profiles: (—△—), A/phenolic CS303; (—O—) A/phenolic CS311 (------) Durestos RA51 control; A = asbestos.

good if Durestos RA51 results are considered. This is not, however, surprising considering the severity of the ablation environment. For purposes of correlation between the results obtained on the test rig and those obtained in service, each rocket motor firing will be discussed in isolation.

The results obtained from firing 1 correlate well with previous rig test results in that the differences in performance of the three asbestos-reinforced phenolic materials is small. The two newer phenolic materials CS303 and CS311 again show slightly higher attack rates (lower virgin material thicknesses),

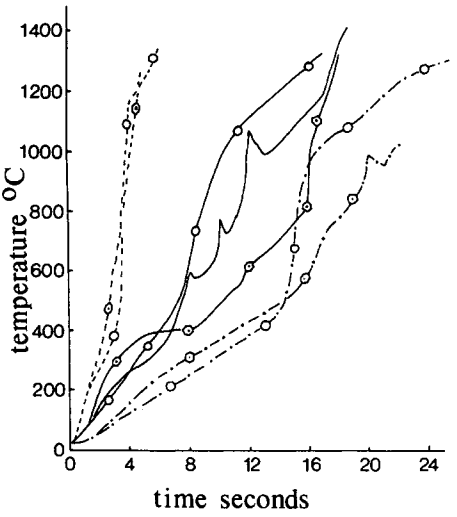

Fig. 12. Tethered rocket time–temperature profiles. Material and thermocouple depth: (---O---) A/polyimide P13N, 0.040 in.; (----⊙----) A/Xylok 210, 0.038 in.; (—O—) A/polyimide P13N, 0.080 in.; (————) Durestos RA51 control, 0.080 in.; (—⊙—) A/Xylok 210, 0.080 in.; (-·-O-·-) A/polyimide P13N, 0.117 in.; (-·-⊙-·-) A/Xylok 210, 0.119 in.; A = asbestos.

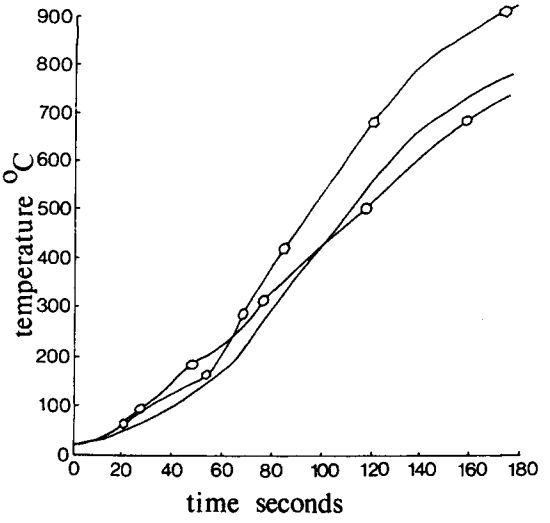

Fig. 13. Ablation test rig time–temperature profiles: (—O—) A/polyimide P13N; (—O—) A/Xylok 210; (————) Durestos RA51; A = asbestos.

with similar erosion rate characteristics. The time–temperature profiles clearly indicate the thermal insulation efficiency of the materials, the different depths of the thermocouples being clearly visible. A time–temperature profile stopping before the end of the firing time indicates that the thermocouple had burnt out. A recorder fault resulted in the loss of two results, 2a and 2c, for the Durestos RA51 control material. It can, however, be seen that the results correlate with the results obtained from the ablation test rig, (Fig. 11), and no obvious anomalies occur.

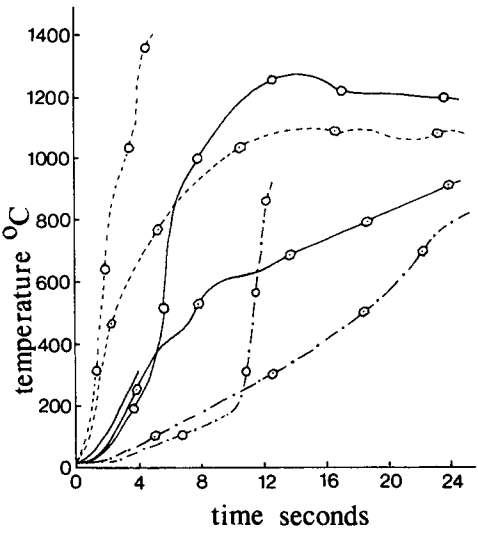

Fig. 14. Tethered rocket time–temperature profiles. Material and thermocouple depth: (----⊙----) Refrasil/resin RA51; 0.026 in.; (----O----) Kaowool/resin RA51, 0.026 in.; (—⊙—) Refrasil/resin RA51, 0.066 in.; (———) Durestos RA51 control, 0.066 in.; (—O—) Kaowool/resin RA51, 0.063 in.; (-·-⊙-·-) Refrasil/resin RA51, 0.103 in.; (-·-O-·-) Kaowool/resin RA51, 0.107 in.

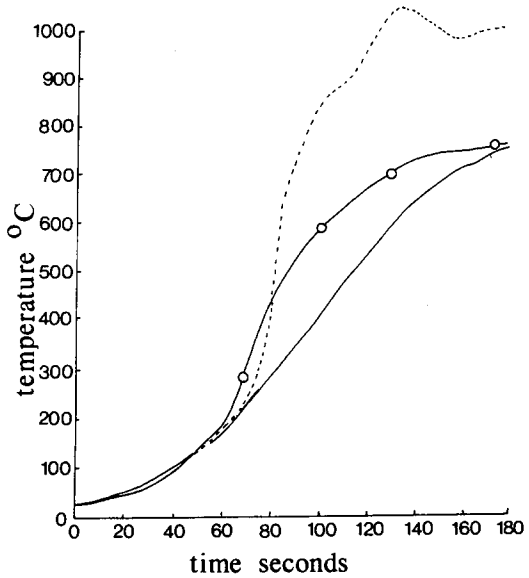

Fig. 15. Ablation test rig time–temperature profiles: (—O—) Kaowool/resin RA51; (------) Refrasil/resin RA51; (———) Durestos RA51 control.

Firing 2 shows a good correlation with the char thickness results previously obtained. The asbestos/polyimide P13N composite gives a very similar performance to the Durestos RA51 control, with the asbestos/Xylok 210 material showing a higher attack rate but similar erosion rate characteristics. The time–temperature profiles agree well with the test rig data shown in Figure 13, and in particular the plateau effect of the polyimide is again clearly defined.

Firing 3, Table V, shows the superior erosion resistance of the Refrasil- and the Kaowool-reinforced RA51 phenolic resin systems. The time–temperature profiles are less conclusive than for the previous two firing. However, nothing is apparent, which contradicts the results obtained on the ablation test rig (Fig. 15).

The results obtained thus correlate well with results obtained from the ablation test rig and on thermal analysis, particularly when the severity of the environment is taken into account. No anomalies occur in the results obtained, and nothing is apparent which contradicts the rig behavior. The field trial results, however, highlight the difficulties of conducting material selection tests using rocket motor firings and show the usefulness of the rapid, low-cost screening test as developed in this work and used in conjunction with the thermoanalytical techniques of TG and DTA.

The authors thank Imperial Metal Industries, Summerfield Research Station, for a Research Studentship (to D.K.), and for the field trial results, and thank Mr. M. J. Chase for useful discussions.

References

1. D. Kershaw, R. H. Still, and V. G. Bashford, *J. Appl. Polym. Sci.*, **19**, 959 (1975).
2. D. Kershaw, R. H. Still, and V. G. Bashford, *J. Appl. Polym. Sci.*, **19**, 973 (1975).
3. D. Kershaw, R. H. Still, V. G. Bashford, and S. J. Hurst, *Chem. Ind.*, 95 (1973).
4. American Society for Testing Materials Specification ASTM E 285-70, Standard Method for Oxy-Acetylene Ablation Testing of Thermal Insulation Materials,"
5. F. J. Koubeck, *J. Macromol. Sci.-Chem.*, *A***3**, 395 (1969).
6. I.M.I. Ltd., private communication.
7. C. Z. Carroll-Porczynski, *Advanced Materials*, 17 (1969).
8. N. Grassie and R. McGuchan, *Eur. Polym. J.*, **6**, 1277 (1970).

Received July 25, 1974
Revised September 23, 1974